



EFFECT OF COMBUSTOR DIAMETER ON NATURAL GAS COMBUSTION CHARACTERISTICS

Elzallat A. M.*¹, Farag T. M.², Gad H. M.³, Ibrahim I. A.⁴

*^{1, 2, 3, 4}Department of mechanical power engineering, Port Said university, Egypt

KEYWORDS: Combustor geometry, Combustor diameter, Air swirler, Combustion modeling

ABSTRACT

This paper represents a numerical study on the effect of combustor diameter on natural gas combustion characteristics. The numerical simulation of a non-premixed natural gas flame has been performed in a three dimensional combustor model. CFD studies were carried out using ANSYS FLUENT 14.5 code. The effect of changing the combustor diameter is studied under different operating conditions of air swirl numbers and excess air factors where two swirlers with $S = 0.5$ and 1.5 are used at $\lambda = 2$ and 4 at constant natural gas fuel mass flow rate of 0.4 g/s. The obtained results from the simulations are presented to clarify the effect of the studied geometrical parameter on combustion characteristics such as axial velocity distribution, reverse flow zone (RFZ), flow pathlines, vortex eye location, recirculated flow mass ratio, temperature distribution and concentration percentage of combustion products. The results show that the length of the central reverse flow zone (CRFZ) increased by increasing combustor diameter in addition to increasing the recirculated flow mass ratio while the average outlet temperatures and the average concentrations of CO and unburnt CH₄ at combustor outlet are decreased.

INTRODUCTION

Combustion chamber manufacturing is one of the most important stages in gas turbine industry. Proper combustor design is critical to establish maximum unit performance, longest life time and to meet the environmental regulations. The combustor had to be designed according to strict principles to achieve several demands like high combustion efficiency, wide flame stability limits, low emissions of smoke and gaseous pollutant species, small physical size and weight and complete combustion of the fuel [1, 2].

The design and analysis of combustor geometry are based on combined theoretical and empirical approach so several studies investigated the combustor geometry and its effect on combustion. Chavan R. P. and Mehta H. B. [3] carried out a 2D numerical study of CH₄-air premixed combustion in micro combustors to examine the effects of combustor size, geometry and inlet velocities on the flame temperature. Downscaling the combustion chamber and higher velocities leads to reduction in residence time which results in lower combustion efficiency causing insufficient heat generation unable to maintain the self sustained combustion and when using combustor geometry with a 2D planar channel instead of cylindrical, it leads to higher exit temperature than the cylindrical tube.

A methodology for gas turbine combustor basic design is performed by Conrado A. C. and Lacava P. T. [4]. The idea is to provide information for producing designs that require minimum development time. Criteria for selecting a suitable combustor configuration is examined followed by design calculations using experimental equations for the dimensions of the casing, the liner, the diffuser and the swirler. Calculations of gas temperature in the various zones of the combustor and liner wall temperatures in the presence of film cooling are performed along with design calculations for the dimensions of the air admission holes. A computational program was developed based on these equations.

El-Mahallawy F. and Hassan A. [5] investigated the effect of the exit section geometry and the furnace length on mixing and flow patterns in a cold flow in a industrial furnace. The exit section diameter of the model furnace is varied by using pistons of different inner diameters and mounted at the model downstream end. Different furnace lengths were obtained by adjusting the piston at the appropriate distances from the model inlet. From the results, it is clear that decreasing the exit section diameter has a significant effect on increasing the rate of decay of the primary stream concentration along the model furnace length in addition to decreasing the mixing length that may leads to shorter flames. Also found that reducing the model furnace length has an effect on increasing the rate of decay of the primary stream concentration along the furnace length.

The main objective of the present work is to study the effect of changing combustor geometry on natural gas combustion characteristics under different operating conditions of air swirl number and excess air factor. The geometrical parameter that changed is the combustor diameter. Five combustor diameters ratios of $D_c/D_s = 1, 2, 3, 4$



and 5 are used where D_c/D_s is the ratio between the combustor and swirler diameters. Two swirl numbers $S = 0.5$ and 1.5 are used at $\lambda = 2$ and 4 .

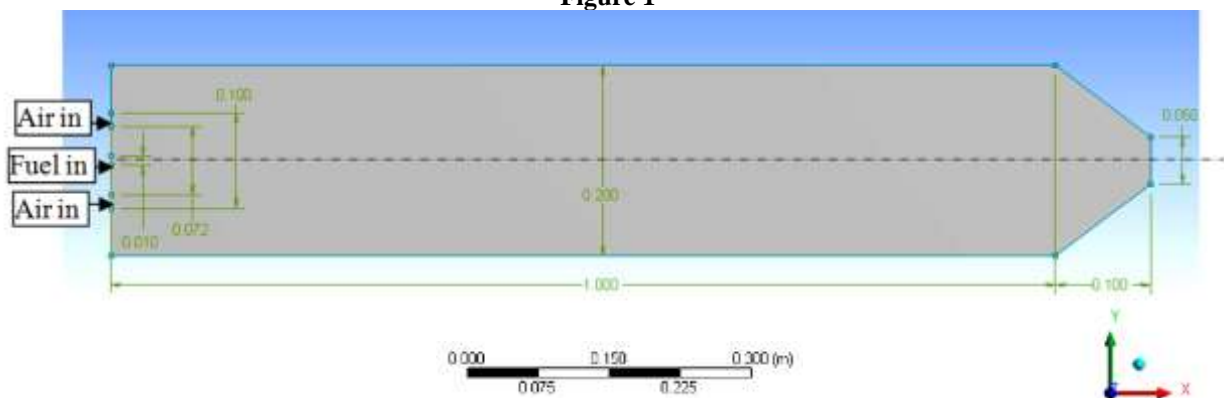
MATHEMATICAL MODEL

In the present work, a CFD analysis for a 3D turbulent swirl combustor is performed using the CFD code ANSYS 14.5, ANSYS is an engineering simulation software used to simulate interactions of all disciplines of physics, structural, vibration, fluid dynamics, heat transfer and electromagnetic. ANSYS are generally comprised of many programs, three of them have been used in this analysis, the first one for geometry (Design Modeler) and the second one for mesh creation (Mesh Generation) and the last one is (FLUENT) for fluid mechanic, heat transfer, chemical reaction and combustion calculations based on the finite volume method.

Physical model

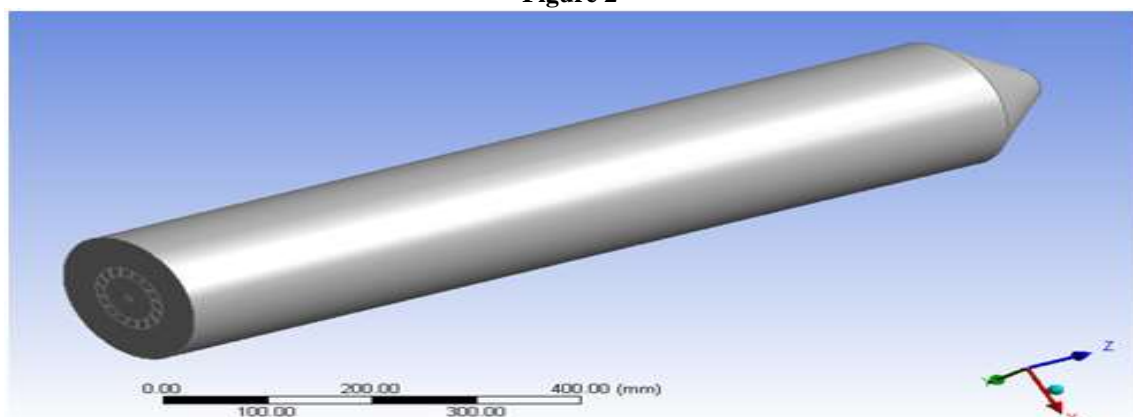
The combustor model that is used as a base for the geometrical changes is a flame tube of 0.2 m diameter and 1 m height with a conical restricted end of 0.1 m height and 0.05 m exit diameter mounted at its top. A circular nozzle of 0.01 m diameter is located at the center of the swirler at the combustor bottom where natural gas is issued axially into the combustor as shown in Figs. 1, 2. Air is introduced through annular swirler having uniform 16 swirl vanes with inner diameter equals 0.072 m and outer diameter 0.1 m. Seven air swirlers having different vane angles of 0° , 15° , 30° , 45° , 60° , 66° and 74° are used to generate swirl numbers of 0, 0.23, 0.5, 0.87, 1.5, 2 and 3, respectively.

Figure 1



Schematic drawing of the base combustor

Figure 2



Geometry of the base combustor model

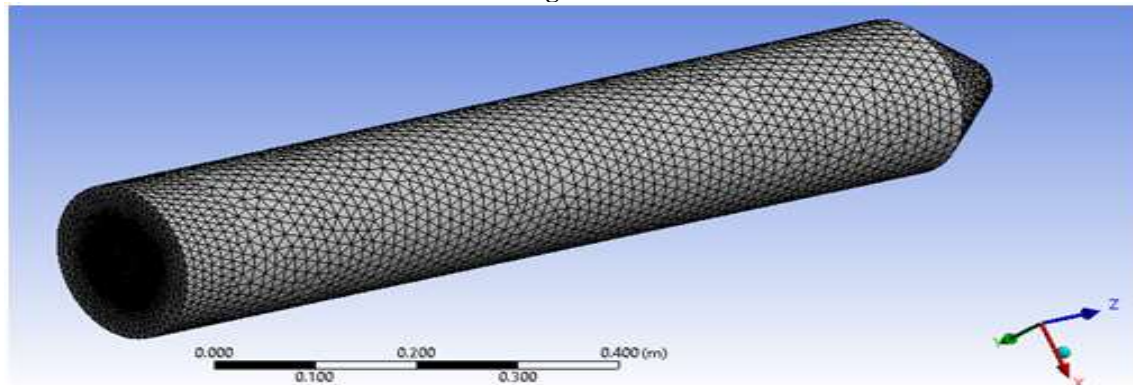
Mesh generation for the model domain

The purpose of meshing is to discrete the model domain into a finite set of control volumes by decomposing the domain into an appropriate number of cells for an accurate result. ANSYS meshing application is used for generating



the mesh. In the present study a unstructured automatic mesh is created where tetrahedrons method with patch conforming algorithm is used as shown in Fig. 3.

Figure 3



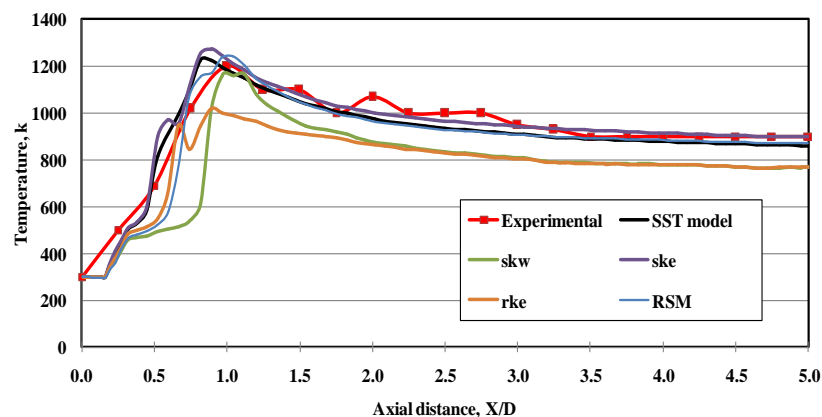
Schematic drawing of the base combustor

Solver settings and physics

Defining solver settings and physics is the last step in the Pre-processor stage of CFD modeling. FLUENT application is the used solver which will be responsible for receiving the generated mesh and settings of the physical models, material properties, domain properties and boundary conditions in addition to defining the convergence controls.

In the present study, a steady state pressure based solver and the energy equation model is enabled since the flow is not hypersonic and there is heat transfer occurs in the system. Also radiation model P-1 is enabled noticing that there are many radiation models but P-1 model can produce a quick and acceptable solution [6]. Several turbulence models are available in FLUENT and by comparing the calculated results using these models with the experimental measurements of centerline axial temperature as shown in Fig. 4, found that the SST k- ω model provided acceptable results that agree with the experimental measurements and are the closest to the RSM model results. Also, less time was consumed for reaching convergent solution when using the SST k- ω model than that when using the RSM model. The SST k- ω model was developed to effectively blend the robust and accurate formulation of the k- ω model in the near-wall region with the free-stream independence of the k- ω model in the far field [7]. Therefore, the SST k- ω is selected for performing further numerical analysis needed for the present study.

Figure 4



Centerline axial temperature at different turbulence models at $S = 0.87$ and $A/F = 50$ ($\lambda = 2.9$)

The non-premixed combustion model is used in the present work for modeling combustion chemical reactions. In non-premixed combustion model, a PDF (Probability Density Function) table is created which contains information on the



thermo-chemistry and its interaction with turbulence. The case study is done at atmospheric pressure and the exit gauge pressure are defined by zero.

Boundary conditions are defined for the physical models zones including the inlet and outlet zones, correct boundary conditions are very important for the accuracy of the CFD solution. The boundary conditions used in this study are given in Table 1.

Table 1. Boundary conditions of the present study

	Zone type	Flow Specification	Turbulence specification	T_{inlet}	Species
Fuel	Inlet mass flow	<ul style="list-style-type: none"> • $\dot{m}_f=0.4$ g/s • Axial velocity component= 1 • Tangential velocity component= 0 	<ul style="list-style-type: none"> • Turbulence intensity= 7% • Hydraulic diameter= 0.01m 	300 k	<ul style="list-style-type: none"> • Mean mixture fraction=1
Primary air	Inlet mass flow	<ul style="list-style-type: none"> • $\dot{m}_a=$Changed as run • Axial velocity component= Changed as run • Tangential velocity component= Changed as run 	<ul style="list-style-type: none"> • Turbulence intensity= 7% • Hydraulic diameter= 0.028 m 	300 k	<ul style="list-style-type: none"> • Mean mixture fraction=0
Outlet	Pressure outlet	<ul style="list-style-type: none"> • Backflow direction specification: Normal to boundary • Radial equilibrium pressure distribution 	<ul style="list-style-type: none"> • Turbulence intensity= 7% • Hydraulic diameter= 0.05 m 	300 k	<ul style="list-style-type: none"> • Mean mixture fraction=0

The Pre-processor stage ends and solving stage starts after entering the boundary conditions and initializing the solution in FLUENT application then the discretized conservation equations are solved iteratively until reaching convergence. For most problems, the default convergence criterion in FLUENT is sufficient. This criterion requires that the scaled residuals decrease to 10^{-3} for all equations except the energy and the radiation model P-1 equations, for which the criterion is decreased to 10^{-6} [8].

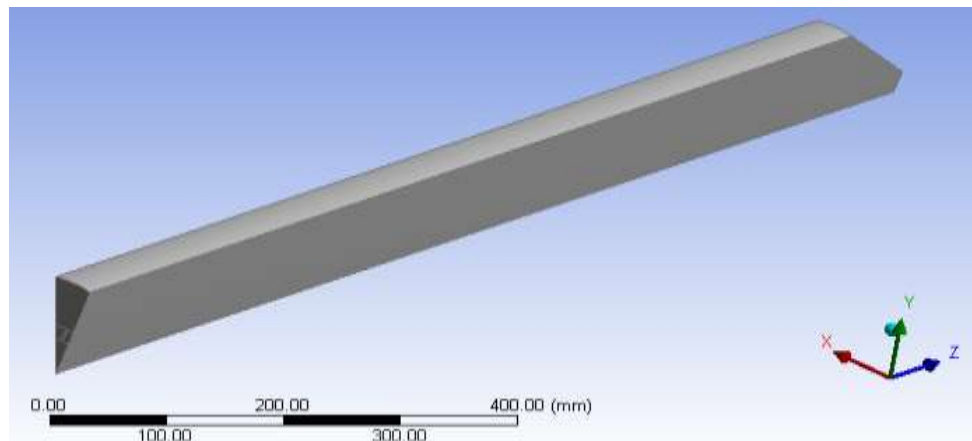
Revision of the model results

In the first simulation trials of the present study, a 2D combustor model was created but the calculated result was overvalued comparing to the experimental measurements. So the simulation carried out in a complete 3D model instead and found that the results are agreeable with the experimental measurements but this was at the expense of computational time and processing speed due to large mesh size. Since the present combustor model has the advantage of symmetry and periodical geometry and the air swirler has sixteen cyclic vanes. Only one sixteenth section of the combustor is modeled using the periodic boundary conditions available in FLUENT to decrease the computational time. By performing analysis, found the calculated results using this section were more accurate than the full 3D model due to the increase of the mesh cell number in the section model compared to the same section in the full 3D model which leads to better accuracy as shown in Figs. 5, 6.

Validation of computation

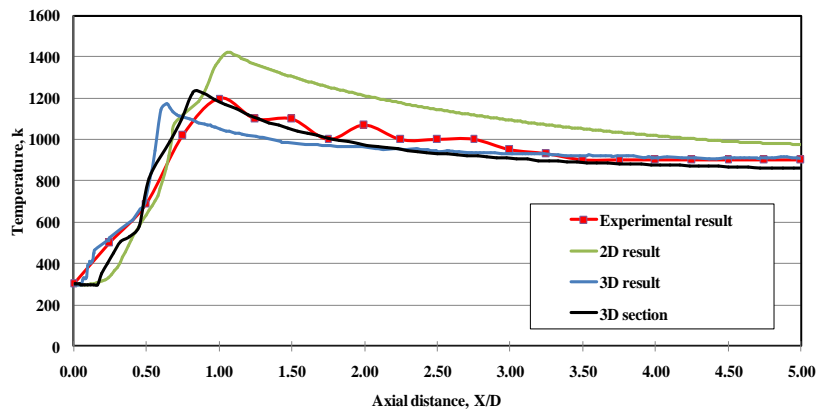
In order to validate the computational procedure, comparison of the present calculations with the experimental data was performed. The experimental data were obtained from a PHD dissertation [9]. The base combustor model that used in the present research for validation has the same geometry of the combustor used in the physical experiments with the same operating conditions but with using the periodic boundary conditions that enables to model only one sixteenth section of the combustor. Comparisons between the experimental data and the calculated results of the centerline axial temperature profiles are shown in Figs. 7 and 8. It is shown that computational analysis has produced agreement between the numerical results and the experimental results.

Figure 5



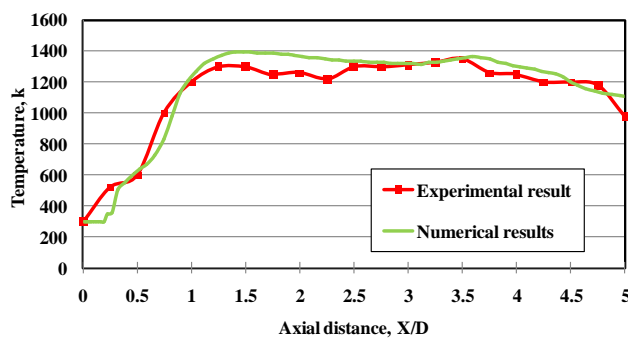
Flow model of the one sixteenth section of the 3D combustor

Figure 6



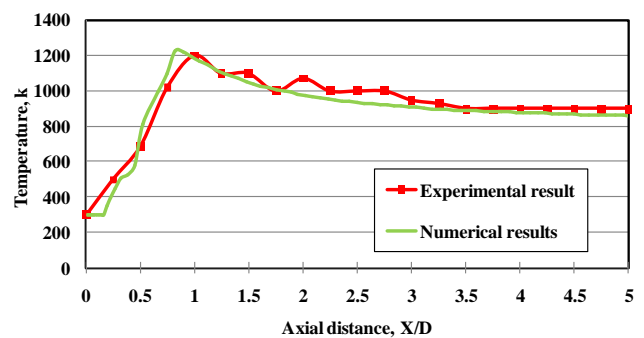
Centerline axial temperature of experimental, 2D, 3D and 3D section models at $S = 0.87$ and $A/F = 50$ ($\lambda = 2.9$)

Figure 7



Comparison between the experimental and calculated results of the centerline axial temperature distribution at $S = 0.5$ and $A/F = 30$ ($\lambda = 1.7$)

Figure 8



Comparison between the experimental and calculated results of the centerline axial temperature distribution at $S = 0.87$ and $A/F = 50$ ($\lambda = 2.9$)

RESULTS AND DISCUSSION

A. The effect of combustor diameter on flow pattern with combustion

The effect of combustor diameter on natural gas combustion characteristics is investigated. Five combustor diameters are used ($D_c/D_s = 1, 2, 3, 4$ and 5 where D_c/D_s is the ratio between the combustor and swirler diameters where the swirler and the end restriction diameters are kept constant at 0.1 m and 0.05 m respectively. Two swirlers at $S = 0.5$ and 1.5 are used at $\lambda = 2$ and 4 at constant natural gas fuel mass flow rate of 0.4 g/s.

1. Effect of combustor diameter on axial velocity distribution (Axial velocity map)

Increasing combustor diameter is highly affecting the distribution of the axial velocity inside the combustor. At weak swirl as $S = 0.5$, the size of the reverse axial velocity region at the combustor centerline increased in length and diameter by increasing combustor diameter while at $S = 1.5$, the size of the reverse axial velocity region at the combustor centerline increased in diameter but the length is almost constant as shown in Figs. 9 and 10. Increasing the combustor diameter at $S=1.5$ leads also to increase the size of the fuel flow penetration inside the CRFZ while at $S = 0.5$, the size of the fuel flow penetration inside the CRFZ is almost constant. This may be attributed to the shifting of the region of the high negative axial velocity region in the CRFZ from the combustor centerline in front of the fuel flow as in $S = 0.5$ case to be above the centerline near the combustor wall as in $S = 1.5$ case. In addition the levels of the forward axial flow velocity outside the CRFZ are decreased by increasing the combustor diameter.

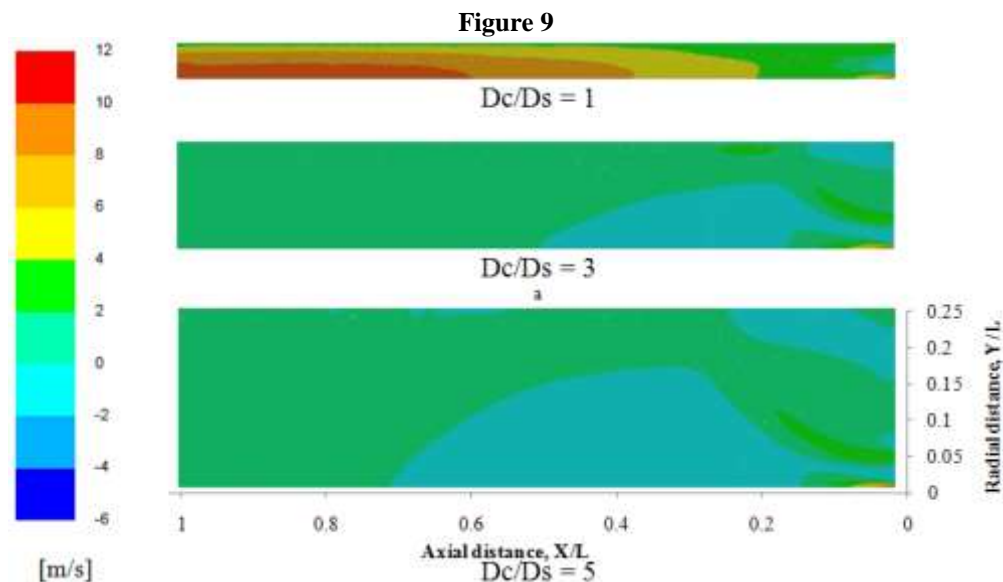
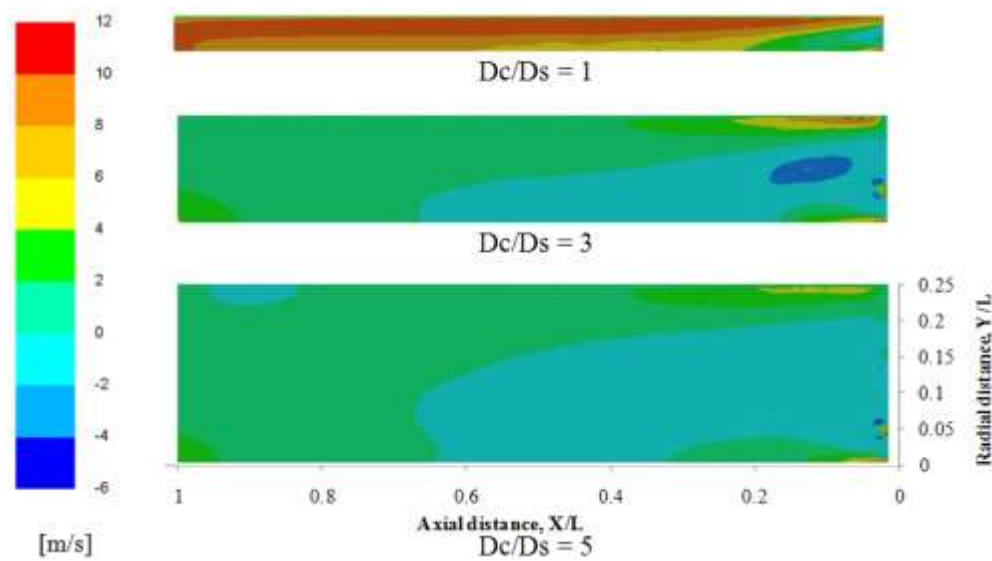


Figure 10



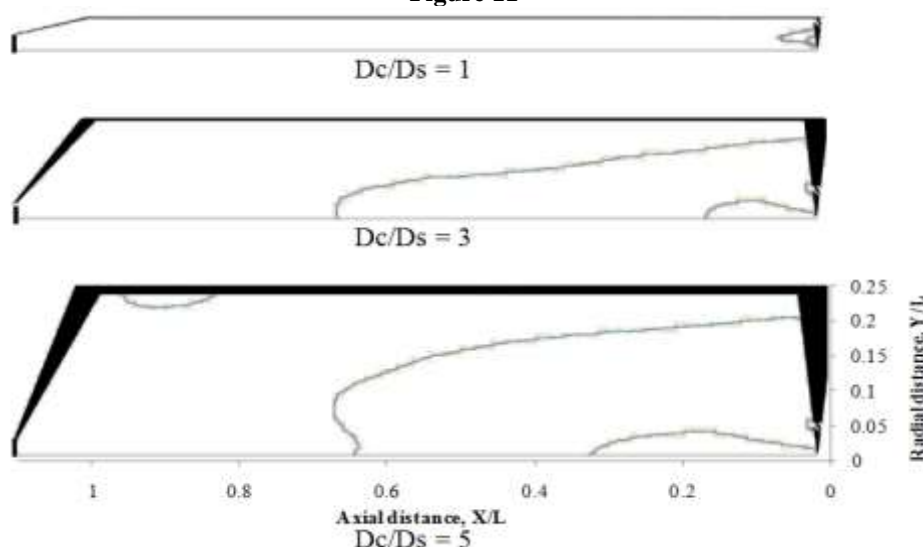
Effect of combustor diameter on axial velocity at $S = 1.5$ and $\lambda = 4$

2. Effect of combustor diameter on RFZ boundary

Combustor walls has a major role in creating the CRFZ, the combustor walls redirects the air coming from the swirler to flow around the CRFZ confining it then due to the combustor end restriction effect, the flow is directed to the combustor centerline axis leading to the breakdown of the CRFZ at the stagnation point. As shown in Fig. 11, at $D_c/D_s = 1$ only a small CRFZ created attached to the combustor core wall and by increasing the combustor diameter, the CRFZ gets larger due to the longer distance traveled by air coming from the swirler before being redirected by the combustor walls, the same effect found at different operating conditions except that at high swirl numbers as $S = 1.5$, the size of the CRFZ increases in diameter but the length is almost constant and also the combustor diameter increase leads to increase the size of the fuel flow penetration.

By increasing combustor diameter further more than $D_c/D_s = 5$, the CRFZ are collapsed due to the moving away of the walls from the combustor centerline. The present work is focusing on studying the effect of combustor diameter until $D_c/D_s = 5$ before reaching the stage of CRFZ collapse.

Figure 11

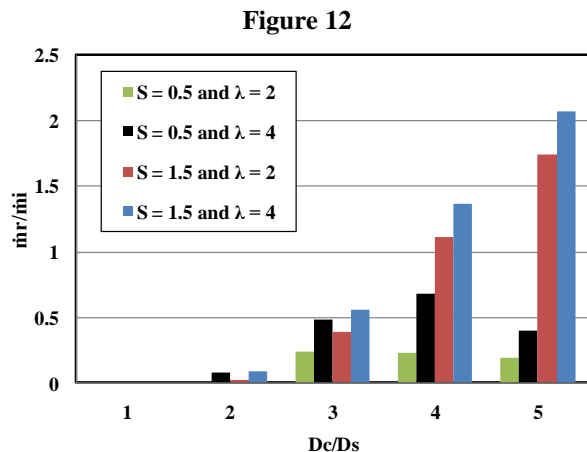


Effect of combustor diameter on RFZ boundary at $S = 1.5$ and $\lambda = 4$

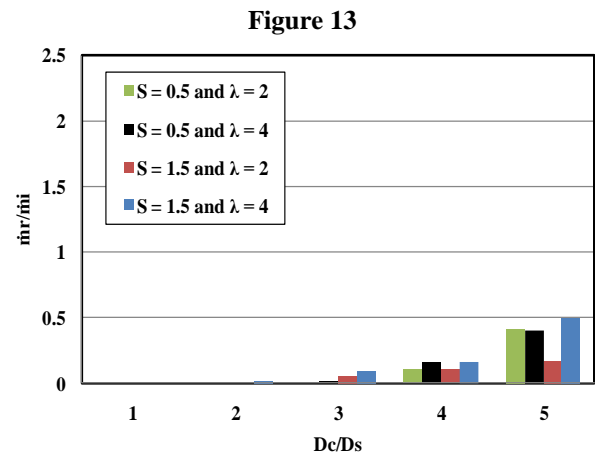
3. Effect of combustor diameter on recirculated flow mass ratio

The mass ratio of the recirculated flow inside the recirculation zone to the mass of the inlet flow is calculated at two

sectional surfaces at axial distances $X/D = 1$ and 2.5 at the combustor model where D is kept constant at 0.2 m in the calculation of the axial distance. Generally the recirculated flow mass ratio is increased with increasing the combustor diameter but when increasing the diameter further than $D_c/D_s = 3$ at $S = 0.5$, the mass ratio started to decrease at section $X/D = 1$ because the CRFZ getting longer and thinner at this section which leads to less reversed mass flow as shown in Fig. 12 and 13.



Effect of combustor diameter on recirculated mass flow ratio at $X/D = 1$



Effect of combustor diameter on recirculated mass flow ratio at $X/D = 2.5$

4. Effect of combustor diameter on flow pathlines

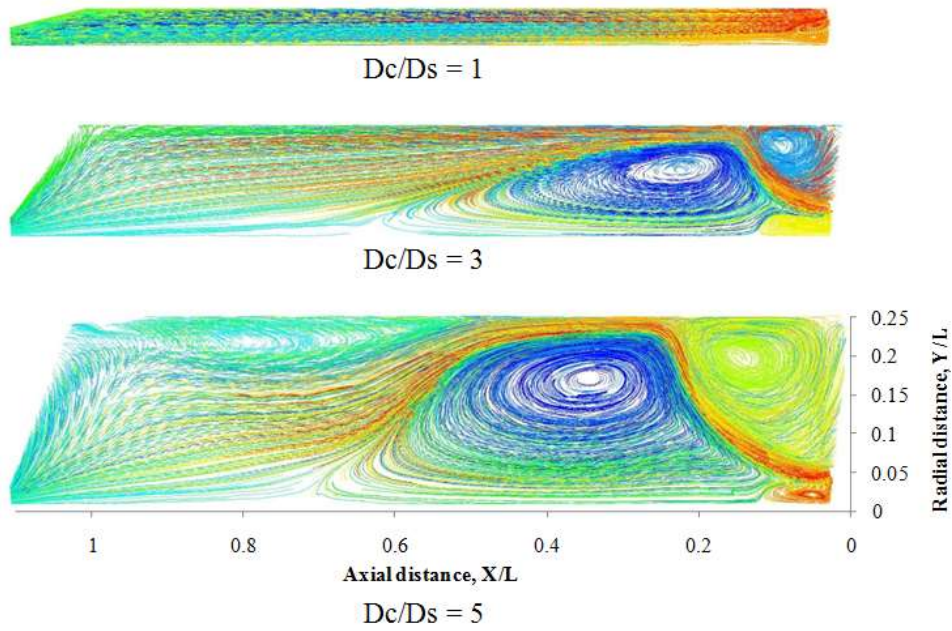
Flow pathlines is used in the present work to visualize the motion of the swirling flow including the recirculation zone and the RFZ indicating the location of the vortex eye. Pathlines are the lines traveled by neutrally buoyant particles in equilibrium with the fluid motion and they are an excellent tool for visualization of complex three-dimensional flows. Pathlines are drawn by ANSYS FLUENT program using the velocity relative to the cell zone motion. The resulting pathlines follow the streamlines based on relative velocity. By default, the pathlines are colored by the particle ID number which means that each particle's path will have a different color [8].

By increasing combustor diameter, the size of the vortex flow of the central and corner flow zones are getting bigger at $S = 0.5$ while the size of the vortex resulting from the fuel flow jet is stayed almost constant. At $S = 1.5$, the corner vortex disappeared due to the tangential flow effect while the size of the central vortex and the fuel flow vortex are getting larger by increasing combustor diameter as shown in Fig. 14.

5. Effect of combustor diameter on vortex eye location

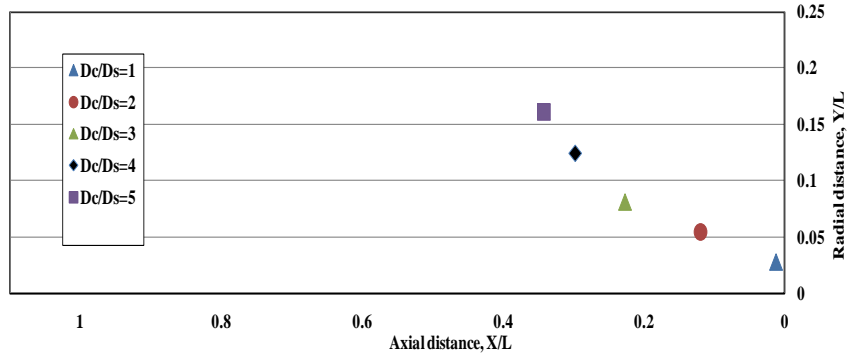
The central vortex eye location shifts gradually downstream the combustor and shifts gradually outward from the combustor centerline axis as a result of the wall movement away of the centerline axis as shown in Figs. 15 and 16.

Figure 14



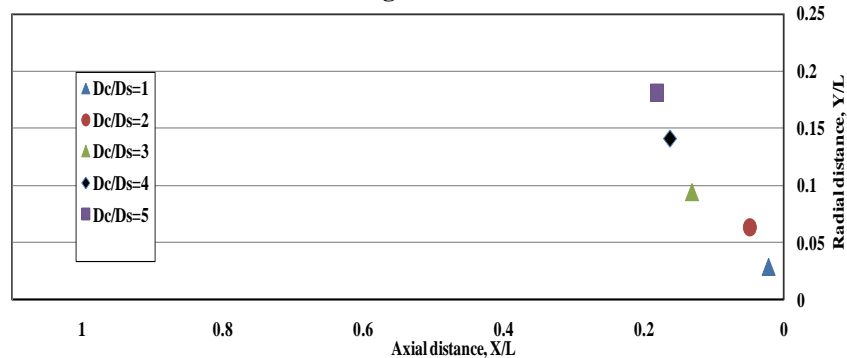
Effect of combustor diameter on flow pathlines at $S = 0.5$ and $\lambda = 4$

Figure 15



Effect of combustor diameter on central vortex eye location at $S = 0.5$ and $\lambda = 2$

Figure 16



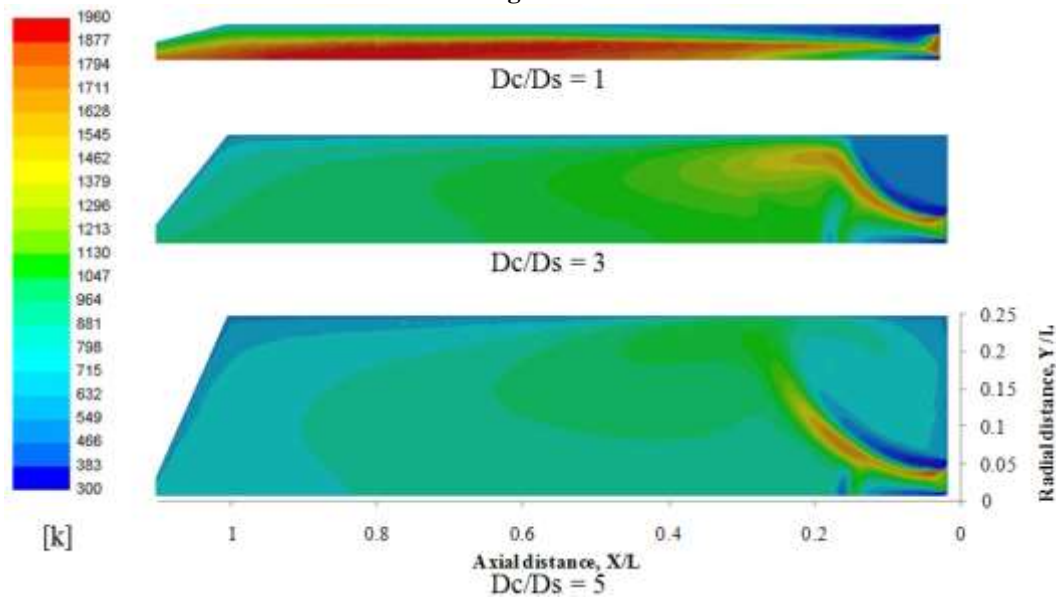
Effect of combustor diameter on central vortex eye location at $S = 1.5$ and $\lambda = 2$

B. The effect of combustor diameter on Temperature Distribution and Species Concentrations

1. Effect of combustor diameter on temperature distribution

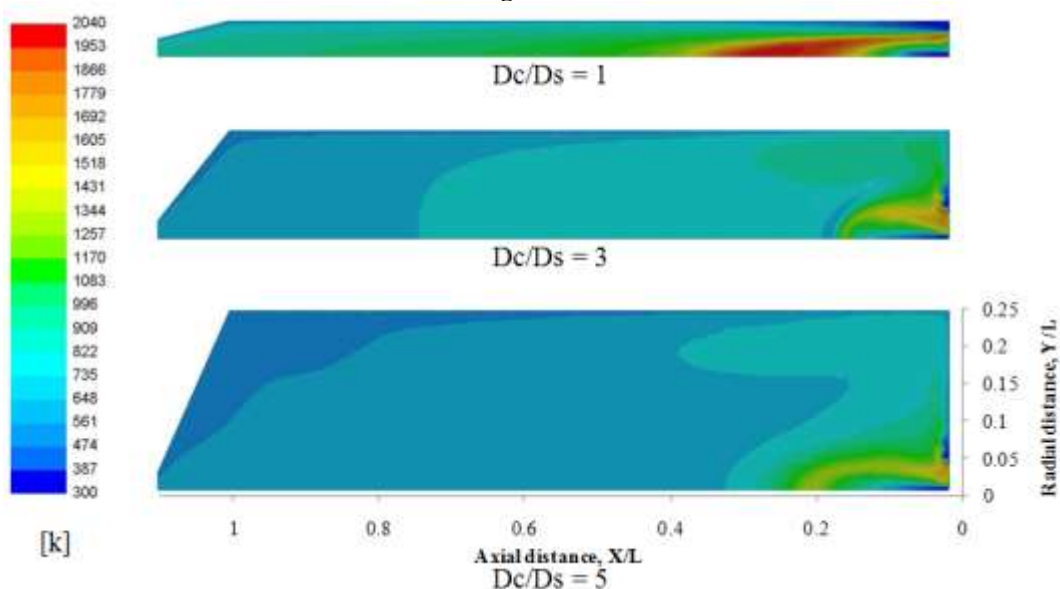
Axial temperatures and average outlet temperature are decreased by increasing the combustor diameter. Also by increasing the diameter, the flame size at weak swirl ($S = 0.5$) gets shorter and inclines against the wall due to the swirling air flow effect and the increase of the CRFZ size. At higher swirl number ($S = 1.5$), the flame base propagates against the combustor wall due to the tangential forces of the swirling flow and also gets longer downstream the combustor due to the increase of the size of the fuel flow penetration as shown in Figs. 17 and 18. The outlet temperature at combustor exit decreased by 35 % and 20 % by increasing the combustor diameter ratio from 1 to 5 at $\lambda = 2$ and 4, respectively as shown in Figs. 19, 20.

Figure 17



Effect of combustor diameter on temperature map at $S = 0.5$ and $\lambda = 2$

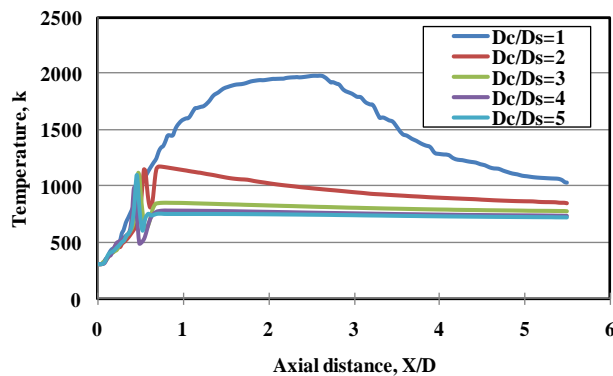
Figure 18



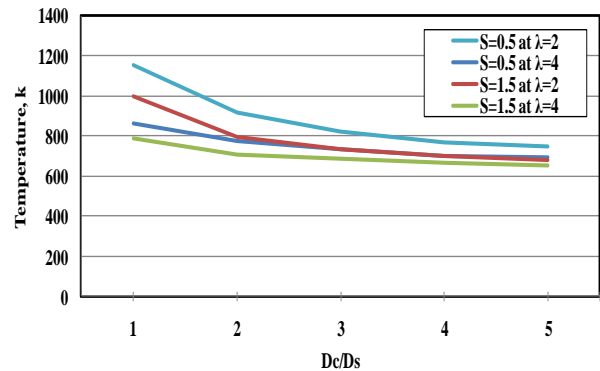
Effect of combustor diameter on temperature map at $S = 1.5$ and $\lambda = 4$

Figure 19

Figure 20



Effect of combustor diameter on temperature at combustor axial centerline at $S = 0.5$ and $\lambda = 4$

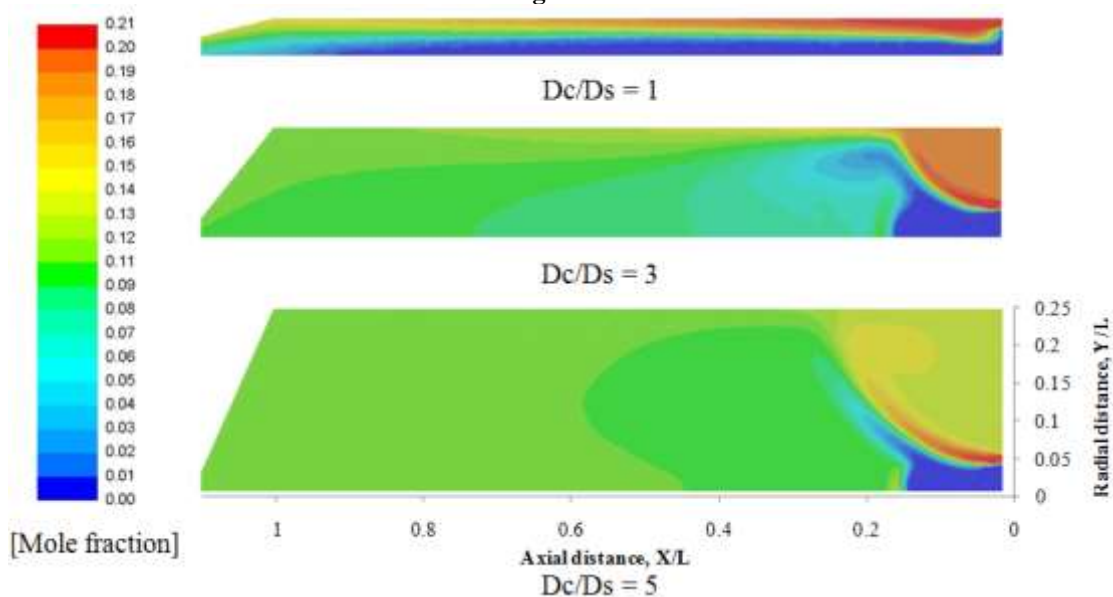


Effect of combustor diameter on average temperature at combustor outlet

2. Effect of combustor diameter on species concentrations

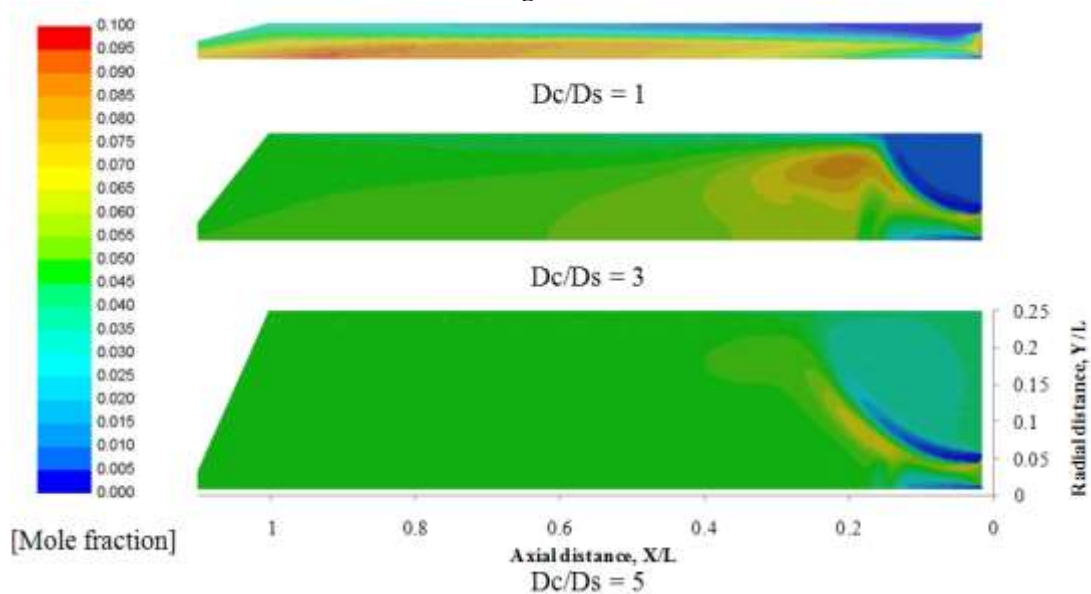
Change of combustor diameter has a great effect on species concentration (CO , O_2 , CO_2 , CH_4) as shown in Figs. 21 to 24. This effect happens due to the change in the temperature distribution and the CRFZ size that leads to the increase of the recirculated mass flow rate and better mixing of air and fuel and consequently complete combustion of fuel which results that the CO and the unburnt CH_4 concentrations at combustor outlet decrease with increasing combustor diameter. The average CH_4 concentration at the combustor outlet decreased by 98 % by increasing combustor diameter from 1 to 3 at $S=0.5$ and $\lambda = 2$.

Figure 21



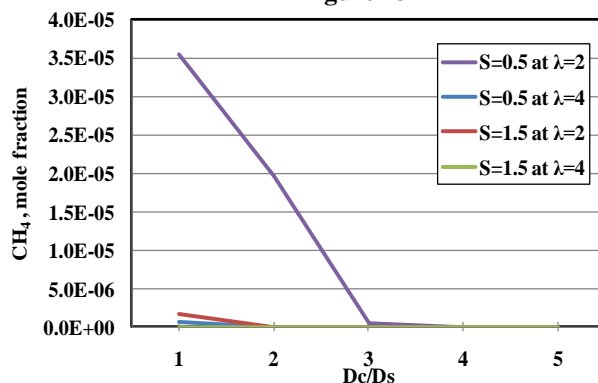
Effect of combustor diameter on O_2 concentration at $S = 0.5$ and $\lambda = 2$

Figure 22



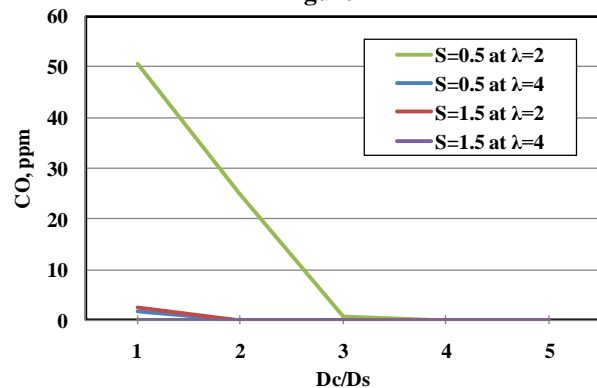
Effect of combustor diameter on CO2 concentration at $S = 0.5$ and $\lambda = 2$

Figure 23



Effect of combustor diameter on average CH₄ concentration (mole fraction) at combustor outlet

Figure 24



Effect of combustor diameter on average CO concentration (ppm) at combustor outlet

CONCLUSION

The effect of combustor diameter on combustion characteristics is studied at $S = 0.5$ and 1.5 with $\lambda = 2$ and 4 . The following results are obtained by increasing the combustor diameter:

- The length of the CRFZ is increased.
- The recirculated flow mass ratio is increased.
- The size of the central vortex is increased and its eye location shifts gradually downstream the combustor and outward from the combustor centerline axis.
- Axial temperatures and average outlet temperatures are decreased. The outlet temperature is decreased by 35 % and 20 % by increasing the combustor diameter ratio from 1 to 5 at $\lambda = 2$ and 4 , respectively. The flame size at weak swirl ($S = 0.5$) gets shorter and inclines against the wall, at higher swirl number ($S = 1.5$), the flame base propagates against the combustor wall and gets longer downstream the combustor.
- Average CO and unburnt CH₄ concentrations at combustor outlet are decreased.



REFERENCES

1. Chaudhari K. V., Kulshreshtha D. B., Channiwala S.A., "Design and CFD simulation of annular combustion chamber with kerosene as fuel for 20 kW gas turbine engine", International journal of engineering research and applications (IJERA), Vol. 2, pp. 1641-1645,(2012).
2. Lefebvre A. H. and Ballal D. R., "Gas Turbine Combustion Alternative Fuels and Emissions", CRC press, ISBN 978-1-4200-8605-8, (2010).
3. Chavan R. P. and Mehta H. B., "A numerical investigation of premixed micro-combustion of CH₄–air mixture", Proceedings of the 37th National & 4th International Conference on Fluid Mechanics and Fluid Power, India, pp. 1-7, (2010).
4. Conrado A. C. and Lacava P. T., "Basic design principles for gas turbine combustor", Braz. soc. of mechanical sciences and engineering, Rio de Janeiro, Brazil, pp. 1-12, (2004).
5. El-Mahallawy F. M., and Hassan A. A., The First Conference of the Mechanical Power Engineering, Faculty of Engineering, Cairo University, Feb., (1977).
6. Yilmaz I., Tastan M., Ilbas M. and Tarhan C., "Effect of turbulence and radiation models on combustion characteristics in propane–hydrogen diffusion flames", Energy Conversion and Management, Vol. 72, pp. 179–186, (2013).
7. ANSYS Fluent theory guide, (2009).
8. ANSYS Fluent user guide, (2009).
9. Farag A. I. A., "Study of secondary air effect on natural gas combustion characteristics", Ph.D. thesis, Portsaid University, Egypt, (2012).